Electronic-vibrational energy transfer between F centers and OH^- impurities in KBr studied by Stokes and anti-Stokes Raman scattering

E. Gustin, M. Leblans, A. Bouwen, and D. Schoemaker
Physics Department, University of Antwerp (U.I.A.), Universiteitsplein 1, B-2610 Wilrijk (Antwerp), Belgium

F. Luty
Physics Department, University of Utah, Salt Lake City, Utah 84112
(Received 2 February 1996)

In contrast to the well-documented case of F-CN^- pairs, little is known about the electronic-vibrational (E-V) energy transfer between an F-center electron and the stretching mode of a neighboring OH^- impurity. We studied this phenomenon for F-OH^- and F-OD^- pairs in KBr by means of Stokes and anti-Stokes resonant Raman scattering. Using CCD-multichannel detection, we were able to obtain more detailed and reliable data than was the case in previous measurements on this center in KCl. Stepwise $F \rightarrow F_H$ conversion experiments revealed the existence of several F-OH^- aggregate centers with stretching-mode frequencies within ~ 10 cm^{-1} from that of the undisturbed impurity ion. In particular, the stretching modes of the two bistable configurations of the $F_H(OH^-)$ center in KBr were identified. Polarized measurements were not able to distinguish between parallel and perpendicular orientations of the impurity with respect to the F_H defect axis in these configurations. The primary E-V transfer process for both isotopes was characterized by accurately measuring the excitation-power dependence of the population of the vibrational levels. The influence of V-V transfer is negligible, as was verified by variation of the impurity concentration. With the assumption that each excited F_H electron transfers energy to the impurity vibration in its relaxation cycle, the vibrational lifetime of OD^- and OH^- in the F_H center is estimated to be of the order of 100 and 10 ns, respectively. Its isotope effect and its temperature independence suggest that decay into hindered rotations is the relaxation mechanism of the stretch vibration. [S0163-1829(96)03334-6]

I. INTRODUCTION

This paper presents Stokes and anti-Stokes resonant Raman scattering (SRRS and ASRRS) results on the $F_H(OH^-)$ center in KBr, using CCD-multichannel detection. The first paper of this series (Ref. 1, to which we will refer as ''paper I'') discusses infrared-absorption measurements on these systems, while a following paper (Ref. 2, or ''paper III'') will present time-resolved measurements of their electronic relaxation.

In most alkali halides (except in NaBr, NaI, and the lithium halides) the F center exhibits an efficient electronic luminescence after optical excitation with a decay time of the order of ~ 1 μs.[3,4] The presence of a molecular impurity (OH^-, CN^-) in its neighborhood can (partially) quench the electronic luminescence. Due to the observation of both electronic and vibrational luminescence, the electronic relaxation and the electronic-vibrational (E-V) transfer process in the case of $F_H(CN^-)$ could be characterized relatively well, although some fundamental questions remain unanswered. The quenching of the electronic luminescence could be correlated to the transfer of the electronic F-center energy to the stretch vibration of the CN^- impurity (E-V transfer).[5] An overview of this work can be found in Ref. 6.

In hosts with the NaCl structure, the quenching of the electronic luminescence is much more efficient when the F center is aggregated to the OH^- impurity.[7,8] The OH^- impurity is positioned on a $\langle 200 \rangle$ position relative to the F center, in units of the interatomic distance.[9–11] For the aggregate $F_H(OH^-)$ center in KCl and RbCl, a fast relaxation component with a time scale of about 3 ps was attributed to electronic relaxation, due to a crossover process.[12] In contrast to the radiative relaxation of the CN^- stretch vibration on a millisecond time scale,[6,13] the intramolecular vibration of the unperturbed OH^- impurity decays nonradiatively in a few nanoseconds.[14] This has been attributed to the decay of the vibrational motion into librational modes. It could be demonstrated that also in the KCl:$F_H(OH^-)$ case there is at least a contribution of E-V transfer to the electronic relaxation, by using anti-Stokes resonant Raman scattering.[15] With this technique a laser beam resonantly excites the F_H-center electron. The Stokes and anti-Stokes resonant Raman scattering (SRRS and ASRRS) of the same beam is then used to measure the stationary distribution of the OH^- over the molecular vibrational levels that was induced by E-V transfer. The measurement of the primary-transfer efficiencies to the different vibrational levels is important, since the efficiencies are determined by the mechanism of nonradiative relaxation and by the interaction between the stretch vibration of the impurity and the F-center electron. The populations of the vibrational levels of the $F_H(OH^-)$ and $F_H(OD^-)$ center in KCl derived by ASRRS, were fitted to a theoretical model, in which the impurity was assumed to act as a promoting mode for the nonradiative relaxation of the electron through dipole-dipole interaction.[15] However, the observed effect upon $OH^- \rightarrow OD^-$ isotope substitution could not be explained in this way. Also, that work was done with high pulsed laser power (~ 1 W average power) because of

the weakness of the ASRRS effect and the usage of photomultiplier detection. High excitation powers have several drawbacks, as will become clear in Sec. V A.

The $F_H(OH^-)$ center in KBr has the particular feature that two different configurations exist, which are bistable below 4 K, and have different electronic absorption characteristics. After cooling from room temperature to 4 K the absorption band is blue-shifted (588 nm) with respect to that of the unaggregated F center (601 nm). It can be optically converted into a red-shifted (615 nm) band, and back.[16] Because the absorption bands strongly overlap, this conversion is always incomplete (paper I). We will refer to the configuration which possesses a red-shifted absorption at 4 K as the ''red center'' or ''red configuration'' (R), and to the other configuration as the ''blue center'' or ''blue configuration'' (B). If the temperature is raised again to 10 K and higher, one observes first a return to a blue-shifted absorption, and then a gradual red-shift of the F_H absorption band as the temperature increases above 10 K. The two configurations are essentially different $\langle 100 \rangle$ orientations of the OH^- relative to the F-OH^- axis.[1,11] In paper I, this is discussed in detail.

II. EXPERIMENT

Measurements were performed on a KBr crystal doped with 8×10^{-4} mol OH^- (University of Osnabrück) and on samples containing both OH^- and OD^- (Crystal-growth Laboratory of the University of Utah). One of them contained predominantly OD^- (8.8×10^{-4} mol OD^- and 1.5×10^{-4} mol OH^-), a second one was exactly equally double doped (1.4×10^{-3} mol), and the third one contained much lower but nearly equal OH^- and OD^- concentrations (0.6×10^{-4} mol OD^- and 0.8×10^{-4} mol OH^-). The equal OH^- and OD^- doping is particularly interesting for a comparison between the $F_H(OH^-)$ and the $F_H(OD^-)$ center under exactly the same conditions. The OH^- and OD^- concentrations were determined by measuring the infrared absorption of the stretch vibration.

F centers were created by additive coloration at 650 °C under a K-vapor pressure of 5 mbar. The resulting F concentrations were between 5×10^{16} cm^{-3} and 1.5×10^{17} cm^{-3}. Before they were mounted in the cryostat, the samples were annealed to a temperature of 400 °C and quenched to room temperature. $F\rightarrow F_H$ conversion was performed by exposing the samples to weak 600-nm laser light at a temperature between 230 and 245 K. In crystals with an impurity concentration of the order of 1×10^{-3} mol, a 40-min light exposure with an intensity of the order of 3 $mW\times cm^{-2}$ was used for most of the measurements. By monitoring the quenching of the luminescence,[7,8] and the shift of the optical-absorption bands,[8,16] it was determined that this results in a complete conversion and that the F_2 concentration was kept sufficiently low. In the low-doped samples a 240-min optical conversion with an intensity three times higher was necessary.

The Raman spectra were recorded using a DILOR XY-800 triple monochromator with CCD-multichannel detection. The resolution was 2.5 cm^{-1} or better in all cases. The spikes occurring in the spectra due to CCD detection were eliminated by comparing several scans recorded under exactly the same conditions, rejecting all data points with excessively high values, and averaging the other ones. In this way we were able to reliably detect anti-Stokes signals down to 0.005 counts/s. In such conditions, the integration time applied for a data point is of the order of 20 min for a single scan. Several laser lines of a Kr^+ and an Ar^+ laser were used, as well as a R6G dye laser. Samples were cleaved along $\langle 100 \rangle$ planes. A perpendicular scattering geometry was used, in which the incident light was polarized along a $\langle 100 \rangle$ axis. No polarization analyzer was used for the scattered light, except in the case of the polarized Raman measurements presented in Sec. IV B.

Due to the large difference in the Raman shift of OH^- and OD^- the wavelength of the scattered light can differ by 30 nm for the two species. To verify that any differences in the Raman intensity are not due to a different spectral efficiency of the Raman spectrometer and the detector, we determined the spectral efficiency by measuring the emission spectrum of a calibrated lamp. The spectral sensitivity of the monochromator and the detector makes it more favorable to observe the Stokes scattering with an excitation wavelength shorter than 570 nm and the anti-Stokes scattering with an excitation wavelength longer than 550 nm. In these conditions, the variations of the efficiency remain limited to less than a factor of 2. Since calibration of the stretching modes by means of laser plasma lines turned out to be insufficiently accurate, we used the frequency of the unperturbed impurity line, known from IR data, to derive the exact frequency of the OD^- and OH^- modes of the aggregate centers in the ASRRS and SRRS spectra. Consistent results were found in this way for the Stokes and anti-Stokes frequency of the F_H center modes, and the results are also in agreement with the Fourier transform infrared (FTIR) measurements of paper I.

For most of the measurements we used a helium-flow cryostat, which can be cooled down to 4.0 K. Under resonant excitation, the laser light is strongly absorbed by the F_H center. Eventually it is completely converted into phonons and a lot of heat is dissipated in a very small part of the sample. This implies that the temperature in the laser beam may be considerably higher than indicated by the temperature sensor in the cryostat, which indicates the average sample temperature. The local temperature is therefore determined from the Stokes and anti-Stokes intensity of the phonon spectrum. The local temperature depends on the laser power, the laser wavelength, the average temperature of the crystal, and on the F_H-center concentration. Its power dependence turned out to be quite linear. This allows for a quick check of the local temperature in each experiment at one power setting. For the F-center concentrations used, the temperature increase under 647.1-nm excitation is of the order of 0.1 K mW^{-1}. The values indicated further on refer to the local temperature, unless stated otherwise.

The laser power incident on the sample has been corrected for the losses at the windows of the cryostat. There is an additional complication in determining the laser power in the focus of the *collecting* lens, i.e., the volume from which the Raman scattering signal is detected. The absorption of the light by the sample reduces the laser power in this volume. To avoid this effect as much as possible, we collect the light scattered from a region near the border of the sample,

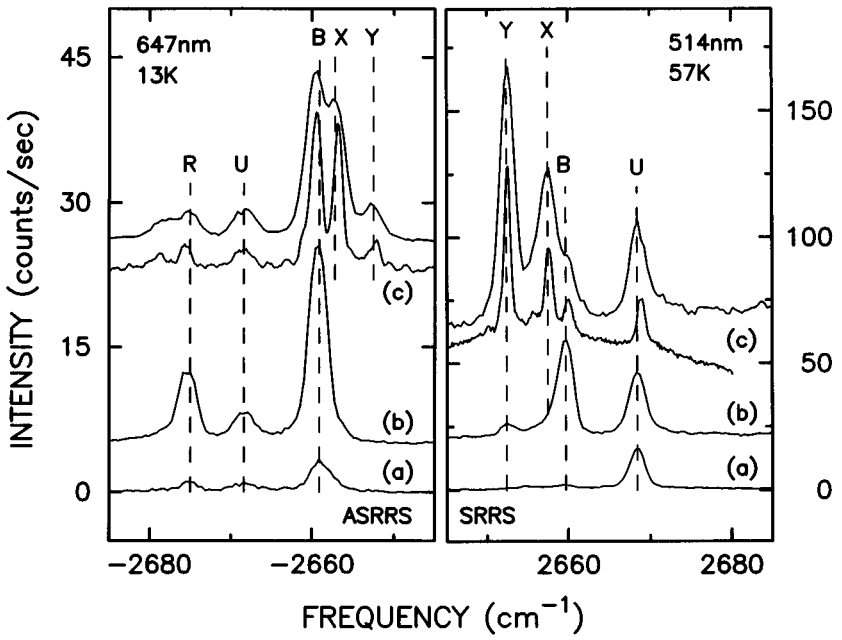

FIG. 1. SRRS and ASRRS spectra in a KBr:OH^-:OD^- crystal, doped with 1.4×10^{-3} mol of each. The SRRS spectrum is recorded at 57 K with 514-nm excitation, the ASRRS spectrum at 13 K with 647-nm excitation. Three stages of $F\rightarrow F_H$ aggregation are presented: (a) Quenched. (b) After an optimal $F\rightarrow F_H$ conversion. (c) After an excessively long aggregation. The lower of the two spectra is recorded with a higher resolution, but with some distortion of the relative amplitudes.

where the laser intensity and thus the Raman signal is largest.

The $OH^-\rightarrow OD^-$ substitution allows one to compare the E-V transfer process of two chemically identical molecules with strongly different vibrational energies (3617.4 and 2668.4 cm^{-1} for the unperturbed OH^- and OD^-, respectively[6,17]). Much of our work was done on samples with equal OD^- and OH^- concentrations. This should allow us to obtain equal concentrations of $F_H(OH^-)$ and $F_H(OD^-)$ centers. The differences between the absorption bands of the $F_H(OH^-)$ and $F_H(OD^-)$ are small (paper I). One can assume in good approximation that the $F_H(OH^-)$ and $F_H(OD^-)$ have the same excitation rate for a given laser wavelength.

III. RAMAN SPECTRA OF THE STRETCHING VIBRATIONS

A. Stepwise $F\rightarrow F_H$ conversion

The perturbation of OH^- or OD^- due to a nearby F center (or any other defect) causes small shifts of the frequency of the stretching-mode vibration. As discussed in paper I, two shifted vibrational absorption lines (B and R) can be identified and attributed to the bistable blue and red configurations. By our Raman experiments we provide an independent confirmation of these attributions, and observe additional vibrational lines.

To identify these lines we performed SRRS and ASRRS measurements of the OD^- stretch vibration after stepwise aggregation. Figure 1 presents Stokes spectra (under 514-nm excitation at 57 K) and anti-Stokes spectra (under 647-nm excitation at 13 K) obtained in the same KBr:OD^- crystal at three different stages: (a) quenched (b) after the optimal $F\rightarrow F_H$ conversion, and (c) after an additional F aggregation with an 18 times stronger illumination. The lower spectrum of the two presented as (c) is recorded under the same conditions as the upper one, but with a three times higher resolution. Apart from the R and B lines associated with the $F_H(OD^-)$ center (paper I), yet unidentified U, X, and Y lines appear. The positions of the lines are listed in Table I. A letter refers to a Raman transition associated with a particular OD^- related defect configuration. If in addition subscripts are used, they indicate the vibrational quantum number of the initial and final state in the Raman transition.

The R and B modes are associated with the two different configurations of the $F_H(OD^-)$ center, observed in electronic absorption,[16] vibrational absorption,[1] and electron-nuclear double resonance (ENDOR) measurements.[11] They are at their maximum with respect to all other modes after the optical conversion used for Fig. 1(b). In the ASRRS spectra the R and B lines associated with the F_H center appear at -2675.0 and -2659.1 cm^{-1}, respectively. This is in agreement with the FTIR results of paper I. Before conversion these modes are weak, because there is only a small statistically formed fraction of F_H centers. Stepwise optical conversion shows that R and B grow with the same amount,

TABLE I. List of $F_H(OD^-)$ and $F_H(OH^-)$ stretching-mode peak positions. The spectra are calibrated by comparing the U line, which appears at the frequency of the unperturbed vibration, with data from infrared-absorption measurements. The experimental error is ±0.5 cm^{-1}.

$F_H(OD^-)$ in KBr	0→1	1→2	2→3
R	2675.0	2582.1	2490.8
B	2659.1	2565.7	2473.4
U	2668.4	2575.2	2483.4
X	2657.0	2563.4	
Y	2652.4	2558.5	
Z	2678.2		
$F_H(OH^-)$ in KBr	0→1	1→2	2→3
R	3626.4	3452.5	
B	3603.6	3428.8	3256.3
U	3617.4	3443.3	
X	3600.6	3425.4	

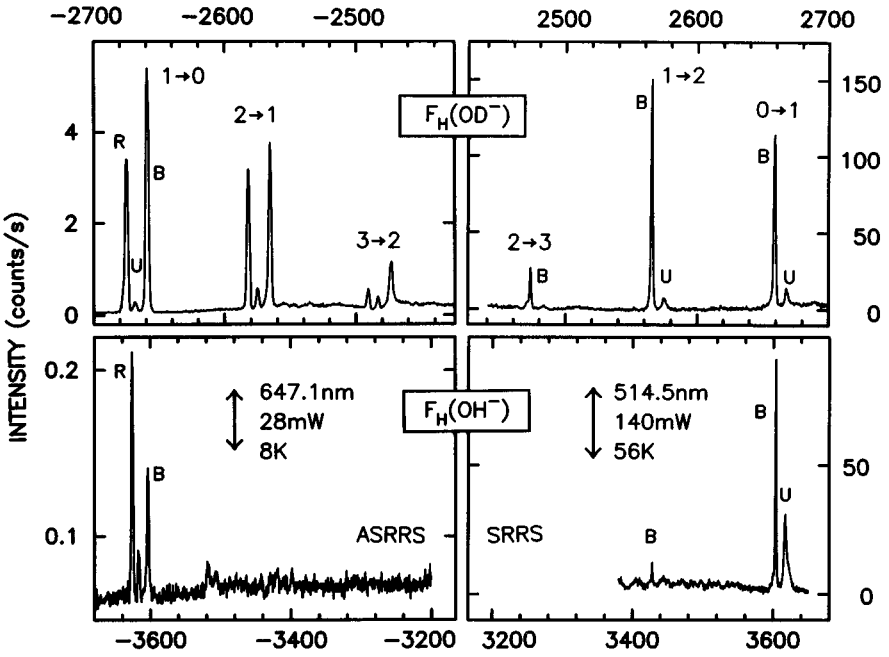

FIG. 2. Typical ASRRS and SRRS for $F_H(OH^-)$ and $F_H(OD^-)$ centers, measured in the same double-doped crystal. The Stokes and anti-Stokes spectra are recorded at a different laser wavelength, excitation power, and temperature, as indicated, but with identical parameters for $F_H(OH^-)$ and $F_H(OD^-)$.

independent of the $v \rightarrow v \pm 1$ transition. This is what one expects for two lines related to the same center. After the optimal conversion of Fig. 1(b) they are an order of magnitude more intense than in the quenched sample. Their relative intensity depends on the temperature and the excitation wavelength (Sec. IV). The SRRS spectra of Fig. 1 have been recorded at a temperature (57 K) and wavelength (514 nm) where the R mode is absent.

The U mode occurs at exactly the same frequency as the vibration of the isolated impurity ion. We verified this by tuning the laser beam in the same experiment from an uncolored sample into a colored one, and from an uncolored surface region of the colored sample into the colored interior part. This showed that within the experimental error (≈ 0.5 cm^{-1}) the $U_{0,1}$ transition for OD^- is found exactly at the frequency of the undisturbed stretching vibration both before and after $F \rightarrow F_H$ conversion (2668.4 cm^{-1}). One expects to observe mainly unperturbed OD^- impurities in a quenched sample, and in the SRRS spectrum of Fig. 1(a) the U line is relatively strongly present. Of course the number of isolated OD^- impurities is, under any condition of conversion, much higher than the number aggregated with F centers. But the large majority of OD^- impurities is not close enough to an F center to have a resonantly enhanced Raman scattering, and their SRRS signal is therefore relatively weak. Under optical conversion, we observe that the U mode increases slightly in the SRRS spectrum. Especially important is that we see it clearly appear in the ASRRS spectrum [Fig. 1(b)], which proves that there is E-V transfer between the F center and the U modes. We attribute this to the creation of ''loose aggregates'' consisting of OD^- impurities at a not too large distance from the F center. This distance must be small enough so that (i) the SRRS of these is resonantly enhanced, and (ii) E-V transfer occurs between the F center and the OD^- ion, causing a strong ASRRS, while the vibrational frequency remains unchanged.

After the very long optical conversion of Fig. 1(c) additional Raman lines appear clearly, which are labeled as X, Y, and Z. The simultaneous decrease of the R and B modes suggests that under excessive aggregation the F_H center is destroyed and more stable aggregates are created. The appearance of the X, Y, and Z modes in ASRRS proves that there is also E-V transfer in these aggregates. They may be F centers bound to a pair of impurity ions. OD^- neighbors at $\langle 200 \rangle$ positions are known to have strongly shifted vibrational frequencies of 2691 and 2655 cm^{-1}. The X and Y modes are close to the latter. Also, the X and Y modes are already weakly present after the optimal conversion in the crystal with an impurity concentration of 1.4×10^{-3} mol [Fig. 1(b)], but they are not observed after optimal conversion in the crystal with much lower (0.6×10^{-4} mol) OD^- doping. The long aggregation also causes a broadening and a shift of the electronic absorption band and the appearance of a shoulder near 540 nm. The Y mode is the strongest one in the SRRS spectrum under 514.5-nm excitation and is only weakly observed in ASRRS under 647.1-nm excitation, whereas the wavelength dependence of X mode is much less prominent. This suggests that the Y mode is related to the additional feature at 540 nm in the optical-absorption spectrum.

B. Population of the vibrational levels

The observation of ASRRS in Fig. 1 shows that the first excited vibrational level of the OD^- stretch vibration is populated by resonant electronic excitation of the F center. Apparently, not only the F_H center is involved in the energy transfer, since also other modes are observed. We are primarily interested in how the F-center energy is distributed over the different vibrational levels of the impurity. Figure 2 presents ASRRS and SRRS spectra for both the OH^- and OD^- stretch vibrations over a broader spectral field, such that also transitions between higher vibrational levels can be observed. The group of Raman lines at the highest Raman shifts are the fundamental vibrational transitions $(v=1) \leftrightarrow (v=0)$ of the different OD^- and OH^- related cen-

ters. It is clear that the Raman spectrum of the OH^- stretch vibration shows similar modes as in the case of OD^- (cf. also Table I). The other groups of Raman lines correspond to transitions $v \rightarrow v \pm 1$ between the higher vibrational levels. For all the observed transitions, the anharmonicity shifts between the fundamental mode and the first overtone lie close to the values (93 and 174 cm^{-1}) observed for isolated OD^- and OH^- defects.[18] It is slightly smaller and larger for the *R* mode and *B* mode, respectively, and it decreases with increasing vibrational quantum number.

The ASRRS and SRRS spectra exhibit some essential differences between OH^- and OD^-. (i) The Raman scattering from the excited vibrational levels is an order of magnitude weaker in the case of OH^-, even though the SRRS from the ground state $v=0$ has a comparable intensity as in the case of OD^-. (ii) With the same excitation power the population of higher vibrational levels relative to that of the $v=1$ level is smaller in the case of OH^- than in the case of OD^-. Whether these observations are related to a faster vibrational relaxation of OH^- than of OD^-, or whether this isotope effect reflects differences in the E-V transfer efficiency, will be discussed in Sec. V.

At temperatures below 30 K a more serious limitation for the observation of Stokes scattering of the stretch vibration is the appearance of a luminescence background. This background has been subtracted in Fig. 2, but it makes the accurate measurement of the weak scattering from higher vibrational levels difficult and SRRS could only be observed with the excitation wavelength at the high-energy side of the absorption band. Therefore, most of the measurements were performed in ASRRS, in spite of the disadvantage that the population of the $v=0$ level cannot be measured.

Although Fig. 2 shows only Raman transitions up to the third excited level, transitions up to the $5 \rightarrow 4$ could be observed under these conditions (Fig. 4). The fundamental question is whether (i) the higher vibrational levels are populated by the primary-transfer process, i.e., due to electronic excitation of F_H centers with the OD^- impurity in the $v=0$ level, or (ii) the vibrational energy is stepwise increased due to repumping of the F_H electron before the OD^- is able to relax vibrationally, as was the case for the ASRRS measurements on the $F_H(CN^-)$ center.[19,20] The power dependence of the ASRRS and SRRS measurements discussed in Sec. V A will answer this question.

C. Electron-phonon coupling

The electron-phonon coupling of an unrelaxed pure *F* center can be determined accurately by measuring the phonon frequency distribution in its SRRS spectrum. In Fig. 3(a) this is shown for a sample containing both OH^- and OD^- in its quenched state, in which basically all *F* centers should be unaffected by the OH^- defects. The spectrum after optical $F \rightarrow F_H(OH^-)$ aggregation (in a sample doped only with OH^-) is shown in Fig. 3(b). Comparison with Fig. 3(a) shows that the SRRS has changed only slightly: The two peaks near 108 and 123 cm^{-1}, representing the optical phonons to which the F center mostly couples, are slightly shifted and broadened. A new band appears near 203 cm^{-1}, well above the limit of unperturbed phonons in KBr.

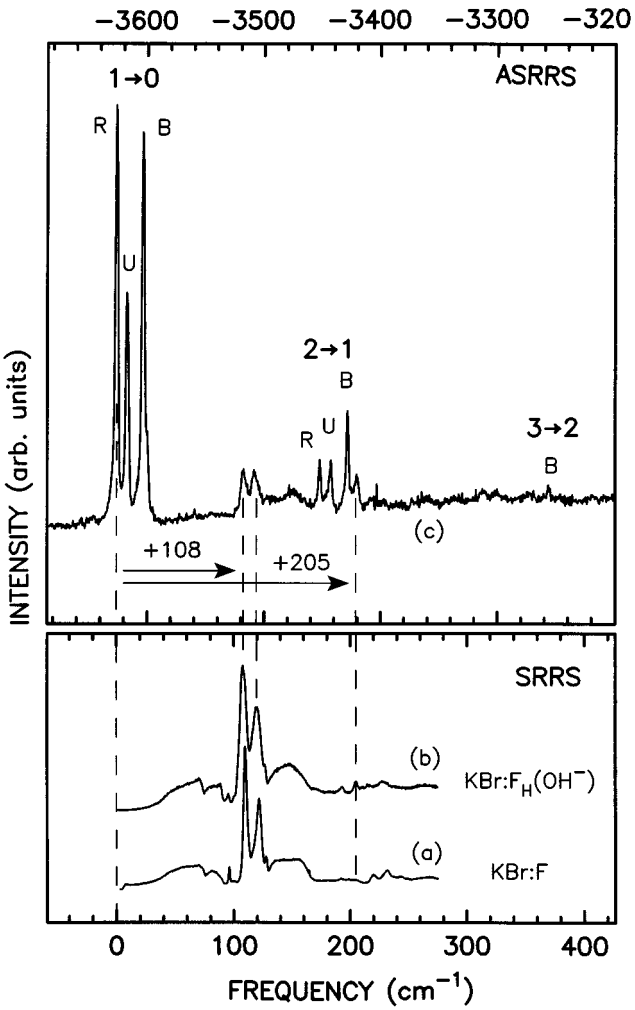

FIG. 3. Comparison of the SRRS phonon spectrum of (a) pure *F* centers and (b) $F_H(OH^-)$ centers. Above this (c) the ASRRS spectrum of its *R*, *U*, and *B* stretching-mode transitions and the observed phonon sidebands. For details of the assignment of the phonon sidebands, see text.

A very similar line appears in the phonon spectrum of the $F_H(OD^-)$ aggregate (Fig. 4). This excludes that this line could be due to some libration or rotation of the ion around its center of mass. The similarity of the phonon spectra for OH^- and OD^- indicates that there is little influence from the molecular ion on the lattice vibrations. In addition, as can be seen from the corresponding ASRRS Raman spectra, also shown in Figs. 3 and 4, there is a great difference in the population of the vibrational levels of the stretching mode for OH^- and OD^-. This too seems to have little effect on the phonon coupling.

As has also been observed for $F_H(CN^-)$ centers in various hosts,[21] phonon sidebands appear at the $v \rightarrow v-1$ modes in the ASRRS spectrum, which are very similar to the low-frequency SRRS spectrum. Figure 3(c) shows this for the OH^- case. The sideband spectrum of the strong $1 \rightarrow 0$ transitions appears between these and the weaker $2 \rightarrow 1$ transitions. In principle, a sideband spectrum can occur for the *R*, the *U*, and the *B* mode. Comparison with Fig. 3(b) shows that agreement between the phonon spectrum and the observed sideband spectrum can only be achieved when shifting the frequency zero-point of the SRRS spectrum (b) be-

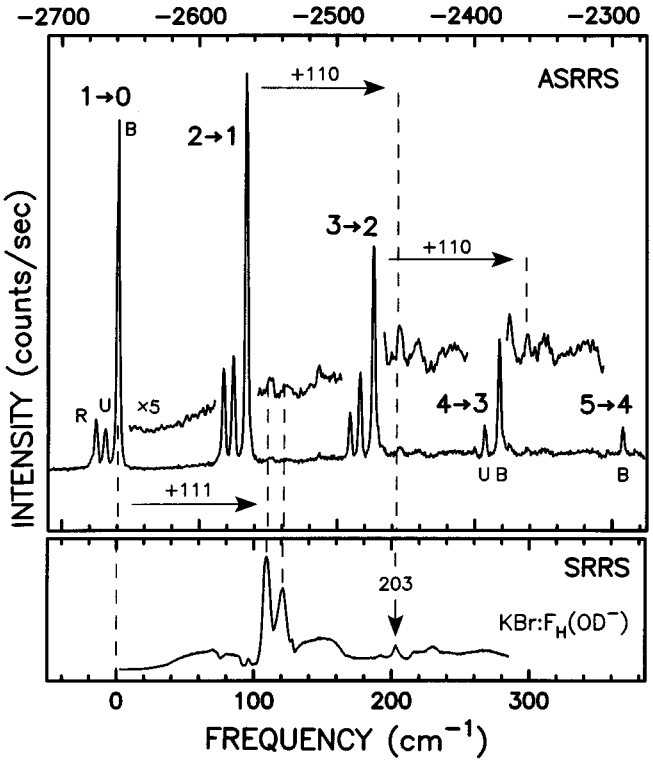

FIG. 4. SRRS phonon spectrum of $F_H(\mathrm{OD}^-)$ centers (lower spectrum) and the ASRRS spectrum of its R, U, and B stretching-mode transitions and the observed phonon sidebands (upper spectrum). The weak sidebands (observable between the stretching modes) are expanded by a factor of 5. For details of the assignment of the phonon sidebands, see text. The ASRRS spectra in this figure and the previous one are obtained in the same crystal, doped with equal amounts (1.4×10^{-3} mol) of OH^- and OD^-, at nearly equal power ($\approx$80 mW) and temperature (12 K).

low the $R_{1,0}$ line of the ASRRS spectrum (c). If sidebands of the U and B modes are present, they must be much weaker. The integrated intensity of the sidebands compares to that of the $R_{1,0}$ mode itself as about 1:1. It is also interesting to note that the extra line near 205 cm^{-1}, relative to the phonon modes near 110 and 120 cm^{-1}, appears to be about 10 times stronger in the sideband spectrum (b) than in the SRRS spectrum (a).

The upper spectrum of Fig. 4 shows the ASRRS spectrum of $F_H(\mathrm{OD}^-)$, in the same doubled-doped KBr:OH^-:OD^- sample as Fig. 3(c), and under nearly identical conditions of excitation wavelength, laser power, and temperature. Because of the higher populations of the higher vibrational levels for OD^- than for OH^-, (Sec. III B) and the near coincidence of the anharmonicity shift and the phonon frequencies, much of possible phonon sidebands of the B, U, and R modes are buried under the next higher $v\rightarrow v-1$ transition. The sidebands that are still visible in the gaps (expanded by a factor 5) can only be attributed to the coupling of the B transition to lattice phonons. Compared to the OH^- case, the ratio of the sideband intensity to that of the vibrational mode itself is an order of magnitude smaller. One may suggest that the sidebands of the R mode might be more intense, but a study of the transitions with a high resolution, in which the stretching-mode vibrations and the possible underlying sidebands can be distinguished because of their different width, indicates that this is not so. The sideband corresponding to the 203 cm^{-1} line overlaps with the phonon-sideband of the $2\rightarrow1$ transition, but by comparing the $2\rightarrow1$ sidebands to the $1\rightarrow0$ spectrum one can conclude that there cannot be a significant contribution from the 203 cm^{-1} sideband. It is therefore possible that the 203 cm^{-1} sideband only appears for the R mode.

IV. OPTICAL AND THERMAL CONVERSION PROCESSES

A. Temperature and wavelength dependence of the F_H center modes

In Sec. III A the R and B modes were associated with the two different configurations of the F_H center. Our association of the R and B stretch vibrations with the red and blue configuration of the F_H center, respectively, was recently confirmed by the FTIR absorption measurements (paper I). At low temperatures, these configurations are stable and can be optically converted into one another. At higher temperatures, a thermal conversion process occurs. There is an important difference between our Raman measurements and the infrared absorption measurements of paper I. In infrared absorption, the concentrations of the ''red'' and ''blue'' centers are determined only by optical conversion in the range $T<10$ K, and by the thermal conversion elsewhere. But in our work the F_H center is excited by the laser beam, which disturbs the thermal equilibrium and makes also unstable configurations detectable. We will study the R and B stretching modes in ASRRS and SRRS, under variation of temperature and excitation wavelength. The behavior of the F_H center under laser excitation is of interest for the time-resolved relaxation measurements, which were done with pulsed laser excitation (presented in paper III).

The temperature dependence of the peak ASRRS intensities of the $R_{1,0}$, $B_{1,0}$, and $U_{1,0}$ modes is presented in Fig. 5 for excitation wavelengths of 647 and 568 nm. The overall ASRRS intensity is larger under 647-nm excitation than under 568-nm excitation, even when taking into account that the efficiency of the spectrometer under 568-nm excitation is only 60% of that under 647-nm excitation. This is true even for the B mode, which is associated with a blue-shifted absorption band. It is possible that excitation in the low-energy tail of the electronic absorption band results in a stronger enhancement of the Raman scattering. The degenerate $2p$ levels of the F center are probably slightly split by the presence of the OD^- impurity ion, so that both the red and blue configuration of the F_H center have an electronic absorption band which consists of several overlapping $1s\rightarrow2p$ transitions. This can produce a wavelength-dependence of the resonant Raman effect, if the $2p$ states couple differently to the vibration of OD^- ion. In addition, the structural differences between the red and blue configurations will result in a different coupling, which could produce a much larger RRS cross section for the blue configuration. The B mode is stronger relative to the R mode under 568-nm excitation than under 647-nm excitation. This is due to a stronger resonant enhancement, because this wavelength is closer to the maximum of the blue-shifted absorption band.

Despite the differences in overall intensity, the temperature dependence is similar for 647 and 568 nm, and we can

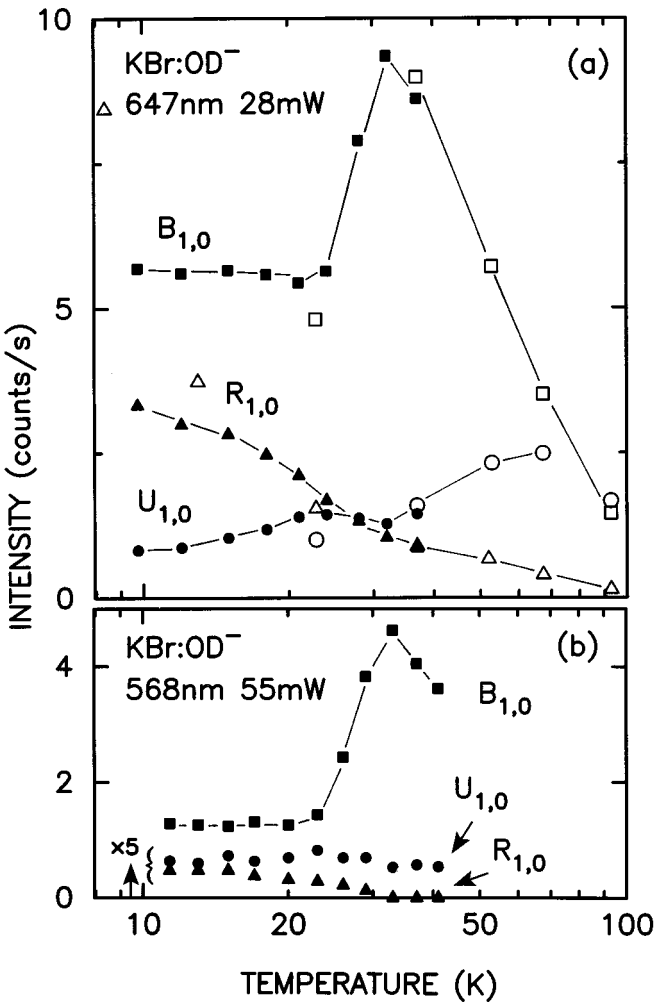

FIG. 5. Temperature dependence of the anti-Stokes stretching mode intensities (a) under 647.1-nm, 28-mW excitation and (b) under 568-nm, 55-mW excitation in the same crystal. The open symbols in (a) represent measurements in another sample. The ASSR intensities of the latter were approximately scaled to compensate for slightly different experimental conditions. Drawn lines are intended as guides to the eye.

distinguish three temperature ranges. Below 25 K the $B_{1,0}$ intensity is nearly constant, while a decrease of $R_{1,0}$ can be observed. The absorption measurements show that at the low end of this temperature range optical bistability occurs and that there is a thermal equilibrium above 10 K. The incident laser light causes an optical conversion, which dominates over the thermal conversion up to 25 K. At this temperature, the thermal and optical conversion rates must be about equal. With the excitation power used, the latter rate is of the order of 10^6 s^{-1} (cf. Sec. V C) taking into account the essentially full quantum efficiency for optical conversion (paper I). Between 25 and 35 K we see a sharp increase of the $B_{1,0}$ intensity, and a corresponding but smaller decrease of $R_{1,0}$. In this region the thermal conversion determines the concentrations, which then become independent of the excitation wavelength. For the $F_H(OH^-)$ case paper I shows that the thermal equilibrium is 2:1 in favor of the blue configuration. For $F_H(OD^-)$ the preference towards blue is even stronger. We also observe that the increase of $B_{1,0}$ is larger under 568-nm excitation ($\times 4$) than under 647-nm excitation ($\times 1.5$). This indicates that the optical conversion favors a smaller number of B centers under 568-nm than under 647-nm excitation. This effect identifies the B mode as associated with the blue-shifted electronic absorption band.

Above 40 K there is a steep decrease of both the $R_{1,0}$ and $B_{1,0}$ modes. The same phenomenon could be observed in vibrational absorption (paper I). Similarly, in ENDOR experiments[11] the F_H center in KBr could not be detected above 20 K. This is in all three cases a reversible process, not related to any destruction of the F_H center. In ASRRS we can also observe the U mode, and we see that it is the only mode which continues to increase in strength with raising temperature, although much more noticeable under 647-nm than under 568-nm excitation. At 90 K, the signal of the $U_{1,0}$ line exceeds that of the R and B modes. The logical conclusion is that at higher temperatures, the F_H center gradually loses its distinguishable R and B configurations, and enters a state which has a vibrational frequency (nearly) identical to that of the isolated OD^-. In particular the vibrational excitation of the K_γ^+ ion, located between the F center and the OH^- impurity, could be important in destroying the bistability effect. A soft mode was associated with the K_γ^+ vibration,[11] which can easily be excited at relatively low temperatures. The observed ''U mode'' at high temperatures thus may become the sum of the ASRRS from distant F-OD^- pairs and the ASRRS of F_H centers in this new state. Only the latter contribution increases, and more prominently under 647-nm excitation because the F_H band is shifted to the red at higher temperatures.

One should not regard the presented measurements as a quantitative indication of the relative R and B concentrations as a function of temperature. The effect of the incident laser light on the configurations, the populations of the vibrational levels, and the resonant Raman enhancement, are all strongly dependent on the absorption band shape. Experimentally, we only observe a composite band, which even under the best experimental conditions is a strong mix of red and blue centers (paper I). The shape of this strongly depends on temperature. At low temperatures, this is probably related to strong changes in the thermal equilibrium populations of the R and B centers.[8,16] The insensitivity of the relative $v \rightarrow v \pm 1$ intensities to temperature variations (cf. Sec. V C) seems to indicate that the excitation rate, and hence the absorption at the laser wavelength, are approximately temperature independent below 35 K. At higher temperatures the shapes of the R and B electronic absorption bands change.

B. Polarized Raman spectra

Having identified the two F_H stretching modes with an electronic absorption band, one can try to obtain information on the particular symmetry of these configurations by means of polarized Raman scattering. Measurements were performed for $\langle 001 \rangle$ polarization of the incident light. The Raman scattering was recorded for light polarized parallel $\langle 001 \rangle$ and perpendicular $\langle 010 \rangle$ with respect to the incident laser beam. The results for ASRRS under 647-nm excitation at 20 K and for SRRS under 514-nm excitation are presented in Fig. 6. For all stretching modes the ratio of perpendicular to parallel scattering intensity is zero within 4%. The ab-

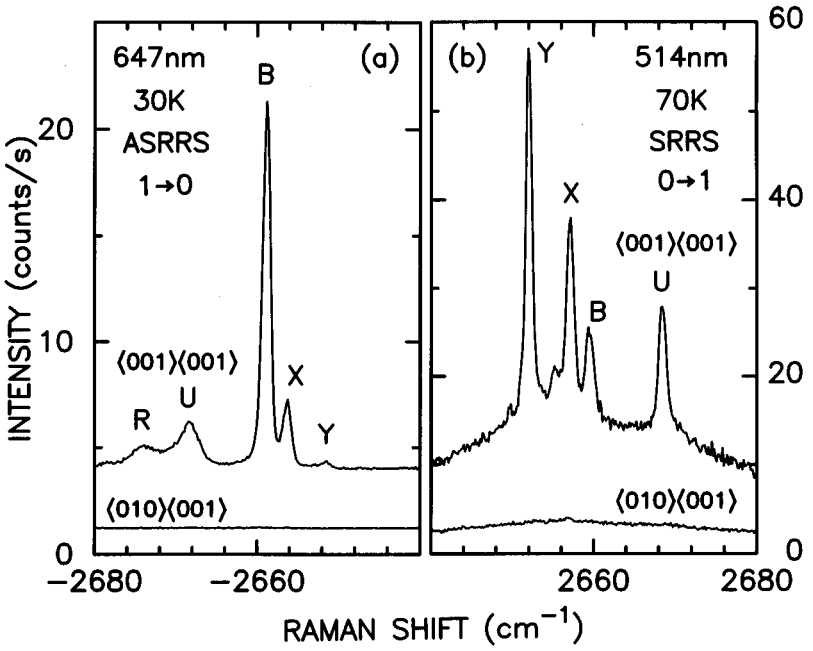

FIG. 6. Polarized Raman-scattering spectra of the $F_H(OD^-)$ center in KBr. (a) Anti-Stokes spectra, (b) Stokes spectra. Due to the temperature (70 K) used for SRRS, the R mode does not appear in the Stokes spectrum. The X, Y, and Z modes are very strong in this spectrum because it was recorded after excessive optical conversion.

sence of perpendicular scattering means that for both the F_H-center configurations the polarization properties are compatible with the C_{4v}:A_1 representation,[22] i.e., the OH^- impurity in a $\langle 200\rangle$ position with respect to the F center and aligned parallel to the defect axis.

In the case of the red configuration this agrees with the ENDOR results. But according to the model of Ref. 11 the OH^- orientation for the blue center is perpendicular to the defect axis, and the OH^- stretching vibration transforms then according to the $C_{1h}(010)$:A' representation. The corresponding Raman tensor possesses also off-diagonal components, allowing both parallel and perpendicular polarized Raman scattering. However, this symmetry determines only that off-diagonal elements *can* differ from zero, but this is not necessarily the case. In resonant Raman scattering, particular elements of the Raman tensors can be enhanced while others are not, depending on the electronic transition resonant with the incident light, and thus on excitation wavelength. The importance of this effect has already been demonstrated for the $F_A(Li^+)$ center.[23] This effect can result in an apparent symmetry increase of the defect. This explanation is even more likely because we see no perpendicular scattering for the X and Y modes, which are attributed to complex aggregates with unknown, but probably lower, symmetry [Fig. 6(b)]. The selective resonant enhancement is expected to be important in particular in the case of resonant excitation of an anisotropic electronic absorption band. Although a single absorption band is observed for each F_H configuration, the threefold degenerate $2p$ state is probably split, so that the band consists of strongly overlapping components with different polarization properties. When in addition the E-V transfer efficiency is dependent on the OH^- orientation with respect to the F center and the incident polarized light, an alignment effect could occur for the vibrationally excited F_H centers. In the case of the anti-Stokes spectra, this can have an additional effect on which Raman tensor components can be observed in the experiment. Polarized Raman measurements by a more systematic variation of the excitation wavelength (hence exciting the different components of the F_H bands) may therefore help to reveal the possible lower symmetry of the blue configuration.

V. E-V ENERGY-TRANSFER PROCESS

A. The primary-transfer process

It is essential for the interpretation to obtain the populations of the vibrationally excited levels due to the primary-transfer process, i.e., the transfer arising from exciting the F center while the molecular impurity is at rest. This assumption is made, e.g., when the experimental data are related to theoretical calculations such as in Refs. 15 and 19. In the case of the RRS measurements on $F_H(CN^-)$ this was clearly not the case.[20] It can be derived from the millisecond vibrational lifetime of CN^-, obtained from vibrational emission,[6,13] that at the laser powers used (10 mW – 1 W) the F_H center is strongly repumped before the CN^- vibration is damped. The repumping is expected to be a less crucial problem in the case of OH^-, because the vibrational lifetime is six orders of magnitude shorter than that of CN^-.[14] However, the vibrational lifetime has only been measured for the *isolated* OH^- defect (3 ns in KBr).[24]

Experimentally, the population of the vibrational levels can be derived from the Stokes or anti-Stokes Raman intensities by means of the formula for a harmonic oscillator:[20,25]

$$I_{v\to v+1}\propto(\omega+\omega_{v\to v+1})^3(v+1)N_vP, \tag{5.1a}$$

$$I_{v\to v-1}\propto(\omega-\omega_{v\to v-1})^3vN_vP, \tag{5.1b}$$

with I the Raman intensity of the transition $v\to v\pm1$ in counts/s, N_v the population of vibrational level v, and P the laser power.

If the E-V transfer is much faster than the vibrational relaxation process (paper III) the steady-state populations of the vibrational levels can be related to the quantum efficiencies η_v of exciting vibrational level v in the primary E-V

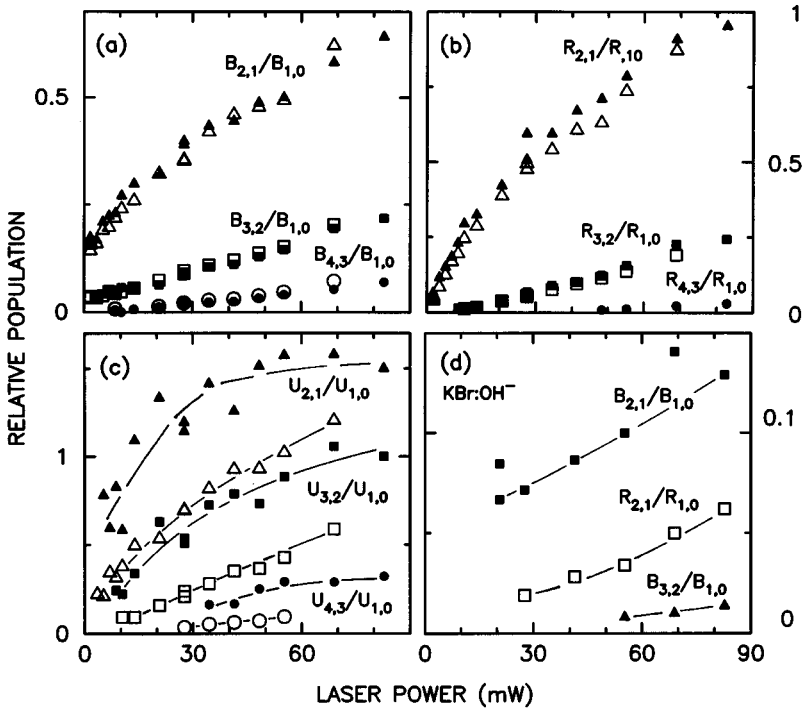

FIG. 7. Excitation-power dependence of the relative populations of the F_H-center vibrational levels under 647-nm excitation. (a), (b), and (c) show the relative populations of the B, R, and U of the $F_H(\mathrm{OD}^-)$ center, respectively. The solid symbols correspond to concentrations of 0.6×10^{-4} mol OD^- and 0.8×10^{-4} mol OH^-, the open symbols to concentrations of 1.4×10^{-3} mol of both. (d) Shows the relative populations of the B and R modes of the $F_H(\mathrm{OH}^-)$ center. Drawn lines are intended as guides to the eye.

transfer process. In the case of SRRS it is convenient to express the populations relative to the population of the $v=0$ level:

$$\frac{N_v}{N_0}=\frac{A}{\gamma_v}\left(1-\sum_{i=0}^{v-1}\eta_i\right), \tag{5.2}$$

in which γ_v is the relaxation rate of vibrational level v and A the electronic excitation rate, which depends linearly on the incident power P. In the case of ASRRS we consider the relative populations with respect to that of the $v=1$ level, because N_0 cannot be determined:

$$\frac{N_v}{N_1}=\frac{\gamma_1}{\gamma_v}\left(\frac{1-\Sigma_{i=0}^{v-1}\eta_i}{1-\eta_0}\right). \tag{5.3}$$

Repumping is avoided as long as $N_v \ll N_0$, which is true when the electronic excitation rate A is much smaller than the vibrational relaxation rate γ_v. Combining Eq. (5.1b) and Eq. (5.2), it is clear that in the primary-transfer regime, N_1 is quadratically dependent on the laser power. This is observed in our system for excitation powers up to 20 mW, which means that we are at least close to the primary-transfer process.

A more stringent criterion for no repumping is that in the primary-transfer process the relative ASRRS intensities [Eq. (5.3)] are independent of the excitation power. Figures 7(a), 7(b), and 7(c) show the dependence of the relative populations of the $F_H(\mathrm{OD}^-)$ modes on laser power under 647-nm excitation, in samples with two different impurity concentrations (0.6×10^{-4} and 1.4×10^{-3} mol). Obviously, the relative populations depend on the excitation power and repumping does occur in spite of the expected short vibrational lifetime of the impurity. In the case of the SRRS under 514-nm excitation (Fig. 2) the presence of repumping is also clear by the fact that the population of the first excited vibrational level is comparable to that of $v=0$. To obtain the distribution over the vibrational levels due to the primary E-V energy-transfer process, we therefore extrapolate the experimental data to zero excitation power. For the blue center the steady-state populations N_v in the primary-transfer regime turn out to be nonzero for $v\leqslant3$. The ratio N_2/N_1 is 0.141 ± 0.005 and $N_3/N_1=0.026\pm0.002$. For the red center only the population of the first excited state is clearly nonzero and N_2/N_1 tends to zero at $P=0$ ($\leqslant0.04$). The power dependence in the case of OH^- is weaker and for the blue center only nonzero populations for $v\leqslant2$ are observed for the primary transfer [Fig. 7(c)]. Under 568-nm excitation only the blue center is strong enough to obtain a reliable power dependence (Fig. 8) and its N_2/N_1 ratio tends to a lower value than under 647-nm excitation.

The transfer efficiencies η_v were estimated by means of formula (5.3), assuming $\eta_0=0$ and $\gamma_v=v\,\gamma_1$. The results are summarized in Table II. A general observation is that the transfer efficiency to the first excited vibrational level is larg-

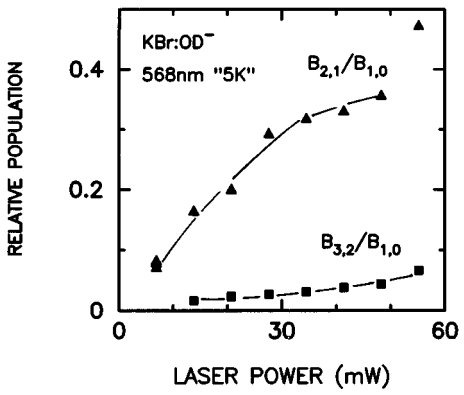

FIG. 8. Excitation-power dependence of the populations of the vibrational levels of the $F_H(\mathrm{OD}^-)$ center, under 568-nm excitation.

TABLE II. Estimated quantum efficiencies for energy transfer in the $F_H(OD^-)$ center. See Sec. V for details on the derivation of these numbers from the experimental data.

	$R(OD^-)$	$B(OD^-)$	$R(OH^-)$	$B(OH^-)$
η_1	~ 1.0	0.72	1.0	0.9
η_2	$\leqslant 0.02$	0.20	0	0.1
η_3	0	0.08	0	0

est in all cases. This is in contrast to the E-V transfer in the $F_H(CN^-)$ center, where the probability is highest to excite the vibrational level most resonant with the emission energy ($v=4$).[6] In the case of the $F_H(OH^-)$ and the $F_H(OD^-)$ center in KBr this would be $v=2$ and $v=3$, respectively, if the emission energy for the F_H center is not shifted too much from the one of the unperturbed F center. Hence, the number of vibrational quanta excited does not match the electronic emission energy of the F center, as was the case for the $F_H(CN^-)$ center.[26]

The transfer efficiency values summarized in Table II should be considered with care, because several assumptions were needed to calculate them. The supposed relationships between the vibrational relaxation rates, $\gamma_v = v\gamma_1$, may not be satisfied. This assumption is valid when the damping of the stretching mode is caused by an interaction, linear in the displacement of the oscillator. This is the case for the radiative relaxation rates of the CN^- molecule for $v \leqslant 6$.[6] Few data are available about the vibrational lifetime of higher vibrational levels of OD^- and OH^-. It is assumed that in these cases, the stretch vibration of the isolated molecule decays into rotations.[14] For OH^- and OD^- impurities in solid Ne and for NH^- impurities in solid Ar γ_2 is about $4\times\gamma_1$.[27,28] If those results give a relevant order of magnitude for the possible deviations from $\gamma_v = v\gamma_1$, Eq. (5.3) still yields the highest E-V transfer efficiency η_1 in most of the cases. Only for the B mode of $F_H(OD^-)$, η_2 and η_1 may be comparable.

This proposed mechanism for the nonradiative relaxation of the stretch vibration raises an additional question on the validity of the values given in Table II. Since the R and B configurations are associated with different orientations of the OH^- in the F_H center, the decay of the stretch vibration into a rotational mode above the rotational potential barrier can imply the following conversion, e.g., a red F_H center in vibrational level v relaxes and has a probability to decay into a blue center in vibrational level $v-1$. In combination with the E-V transfer process, this is a possible explanation for the observed efficient optical conversion between the F_H-center configurations. Alternatively, the relaxation of the stretch modes excites phonon modes, which may include the soft mode of the K_γ^+ ion between the F center and the OH^-, and induce a conversion in this way. Including these red–blue conversion processes in the rate equations could result in some corrections. But because the correction on the population of a level is proportional to the population of the levels above, and the population under primary transfer conditions falls off sharply with increasing vibrational quantum number, the corrections are small. They may be important under conditions of strong repumping.

Another assumption made was that $\eta_0 = 0$. A nonzero η_0 means that a fraction of the electronically excited F_H centers relaxes without transferring energy to the stretch vibration. Since the electronic luminescence is strongly quenched, this would imply that the static perturbations of the impurity ion on the F center are sufficient to produce a high nonradiative electronic relaxation rate with respect to the radiative decay rate. For type(I)-F_A centers and the KCl:$F_H(H_s^-)$, however, the electronic emission efficiency is only slightly affected by the static effects of the impurity.[29] This is also true for KCl:$F_H(CN^-)$,[5] which is probably a more relevant case for comparison with $F_H(OH^-)$ and $F_H(OD^-)$. In host crystals with strong $F_H(CN^-)$ electronic luminescence quenching, the vibrational emission efficiency demonstrates that electronic relaxation is always accompanied by vibrational excitation of CN^-.[26] Nevertheless, it is still important to verify this also for $F_H(OH^-)$ and $F_H(OD^-)$. A nonzero η_0 affects the absolute efficiencies η_v ($v>0$), but not their relative values with respect to each other.

It is possible that after E-V transfer, the vibrational energy is again removed from the system by V-V transfer. Since U occurs exactly at the position of the unperturbed impurity, it is possible that this mode is excited by V-V transfer from vibrationally excited F_H centers. In the case of CN^- this is known to affect the vibrational levels of the F_H center considerably at high impurity concentrations.[26] If V-V transfer is taking place, one expects a concentration effect on the populations of the F_H-center modes, since the efficiency of the V-V transfer is a function of the average distance between the impurities. Measurements with two concentrations, differing by a factor of 20 [Figs. 7(a) and 7(b)], show that there is no concentration effect. The negligible effect of V-V transfer even with high impurity concentrations is not surprising. The V-V transfer rate is related to the radiative lifetime through the dipole transition matrix elements. The nanosecond nonradiative relaxation of the OH^- stretch vibration therefore also suppresses the efficiency of the V-V transfer.[30] At higher temperatures, when the intensity of the R and B modes decreases strongly and that of the U mode rises, the situation is less clear. However, we limit ourselves in this section to low temperatures.

B. Vibrational relaxation and repumping

To analyze the power dependence of the population of the vibrational levels, we include in the model of Sec. V A that a vibrationally excited F_H center can be electronically pumped with an excitation rate A independent of its vibrational state v. The efficiency of the transition from the electronically excited F_H center in the vth vibrational state to vibrational level v' in the electronic ground state, is also assumed to be the same as the primary E-V transfer efficiency $\eta_{v'-v}$ determined in the previous section. We assume again that $\gamma_v = v\gamma_1$. The solution for the steady-state population is then

$$\frac{N_2}{N_1} = \frac{1}{2}\frac{A}{\gamma_1}(1-\eta_0) + \frac{1}{2}\frac{1-\eta_0-\eta_1}{1-\eta_0}, \qquad (5.4a)$$

TABLE III. Vibrational lifetimes τ_v for the stretching mode in the $F_H(OD^-)$ and $F_H(OH^-)$ centers (see Sec. V C for details). The temperature indication of ''4 K'' is used for calculations based on measurements of the power dependence. The local temperature increases with incident laser power at a rate of the order of 0.1 K mW^{-1}. P is the incident laser power, A is the vibrational excitation rate, and γ is the vibrational relaxation rate.

Excitation	F_H center	$\tau_v=\gamma^{-1}$	T	$A\gamma^{-1}P^{-1}$	AP^{-1}
SRRS 7 mW 530 nm	$R(OD^-)$	330 ns	5 K	0.038 mW^{-1}	1.2×10^5 $s^{-1}mW^{-1}$
	$B(OD^-)$	600 ns	5 K	0.056 mW^{-1}	0.9×10^5 $s^{-1}mW^{-1}$
SRRS 200 mW 514 nm	$B(OD^-)$	70 ns	65 K	0.046 mW^{-1}	6.5×10^4 $s^{-1}mW^{-1}$
	$B(OH^-)$	4.6 ns	65 K	0.0003 mW^{-1}	6.5×10^4 $s^{-1}mW^{-1}$
ASRRS 647 nm	$R(OD^-)$	110 ns	''4 K''	0.041 mW^{-1}	3.9×10^5 $s^{-1}mW^{-1}$
	$B(OD^-)$	140 ns	''4 K''	0.018 mW^{-1}	1.3×10^5 $s^{-1}mW^{-1}$
	$R(OH^-)$	7 ns	''4 K''	0.0026 mW^{-1}	3.9×10^5 $s^{-1}mW^{-1}$
	$B(OH^-)$	25 ns	''4 K''	0.0032 mW^{-1}	1.3×10^5 $s^{-1}mW^{-1}$

$$\frac{N_3}{N_1}=\frac{1}{6}\left(\frac{A}{\gamma_1}\right)^2(1-\eta_0)^2+\frac{1}{2}(1-\eta_0-\eta_1)\frac{A}{\gamma_1}+\frac{1}{3}\frac{1-\eta_0-\eta_1-\eta_2}{1-\eta_0}. \tag{5.4b}$$

In the limit of zero excitation power, Eqs. (5.4) are indeed equivalent to the expressions (5.3) for the primary-transfer regime. In spite of the simplifications, formulas (5.4) fit the experimental data of Figs. 7(a) and 7(b) well for excitation powers between 1.7 and 35 mW. At higher laser powers, the predicted populations for vibrational levels higher than $v=1$ systematically exceed the experimental values. At 150 mW, the difference between experimental and theoretical values of N_2/N_1 is more than a factor of 2. The deviations increase with the vibrational quantum number. In view of the approximations made, there may be several reasons for the deviations at high laser power, such as, an electronic excitation rate and an E-V transfer efficiency depending on the vibrational quantum number, $R\leftrightarrow B$ conversion, and a nonvalid $\gamma_v=v\,\gamma_1$ approximation. The latter possibility could not only be caused by the nature of the vibrational relaxation, as explained in Sec. V A. When the vibrational energy is roughly equal to the electronic absorption energy of the F_H center, a V-E back conversion is possible. In the case of the $F_H(CN^-)$ center in CsCl, back conversion processes were suggested to be responsible for the fact that the vibrational levels $v>8$ could not be populated.[31]

Laser powers higher than those displayed in Fig. 7 result in a strong bleaching of the OD^- stretching modes, although the intensity of the SRRS phonon spectrum remains the same. It occurs when the population of the $v=5$ vibrational level is clearly observed. This could be explained in two ways. (i) The F_H center dissociates into an F center and an isolated OD^- ion. At room temperature the F_H centers have a lifetime of the order of hours, indicating that they are not very stable.[7] (ii) The OD^- itself dissociates. It is known that OH^- impurities dissociate and produce interstitial H_0^- centers, when they are electronically excited.[32] The energy necessary for either process to occur may be supplied by energy transfer from a high vibrational level of the OD^- molecule, in the electronic ground or in the electronic excited state of the F_H center.

C. Vibrational lifetime of the $F_H(OH^-)$ center

The population ratio N_1/N_0 in the primary-transfer regime and the ratio N_2/N_1 in the repumping regime are both linearly dependent on the excitation power P with a slope:

$$A(1-\eta_0)\,\gamma_1^{-1}P^{-1}. \tag{5.5}$$

Therefore the vibrational lifetime γ_1 of the OH^- and OD^- stretching mode of the F_H center can be determined, if we assume $\eta_0=0$ and estimate the electronic excitation rate A corresponding to a laser power P. When a laser beam with wavelength λ and power P is focused on the sample to a radius r of about 10 μm, the excitation rate A for a particular F_H configuration (R or B) is given by

$$A(z)=\frac{1}{C}\frac{1}{\pi r^2}\frac{P\lambda}{hc}\mu\exp(-\mu_{\rm tot}z), \tag{5.6}$$

which depends on the penetration distance z. C and μ are the concentration and the absorption constant for that configuration, whereas $\mu_{\rm tot}$ is the total absorption constant. The excitation rates estimated from (5.6) result in the vibrational lifetimes in Table III. They are only an order of magnitude, since A is a difficult parameter to determine exactly. A laser power of 50 mW at 647 nm, e.g., corresponds to an excitation rate $A=(150\ \text{ns})^{-1}$ at the surface of the sample. After 1 mm penetration in a sample with a 1×10^{17} cm^{-3} concentration of B, this rate decreases to less than $(500\ \text{ns})^{-1}$. Raman scattering is collected from a region near the surface, but we do not know its position exactly and within the observed interaction volume the excitation power decreases. Nevertheless, the ratio between the vibrational lifetimes of OH^- and OD^- is reliable, since A is the same in the two cases. The spectra for the different isotopes are recorded in the same crystal (with equal doping) under exactly the same conditions and the absorption bands for $F_H(OH^-)$ and $F_H(OD^-)$ are very similar. Also, the relative values for the vibrational lifetimes for the R and B configurations are reliable insofar as the relative strength of their absorption band can be determined.

We estimated the vibrational lifetimes τ_v in two ways. (i) We calculated it from the ratio N_1/N_0. This can be determined only from SRRS spectra, but it has the advantage that

expression (5.2) for $v=1$ is independent of the assumptions made on the excitation rate, the vibrational lifetime, the transfer efficiencies in the repumping regime, and on complications with the $R \leftrightarrow B$ conversion. However, the scattering from the excited vibrational states is weak compared to the luminescence background in SRRS, because low excitation power must be used for the primary transfer. (ii) From ASRRS spectra the value of $A(1-\eta_0)\gamma_1^{-1}P^{-1}$ was obtained by the fitting of Eq. (5.4) to the power dependence of the population ratios (cf. Sec. V B). The values for τ_v obtained are listed in Table III. The most notable result is that the lifetime for OD^- is an order of magnitude larger than for OH^-. Temperature variation at a constant excitation power in the repumping regime for the ASRRS intensities shows that the relative populations of the vibrational levels are essentially independent of temperature. According to Eq. (5.3) this means that the vibrational lifetime of the stretching mode is temperature independent below 30 K for the R configuration and below 90 K for the B configuration.

The reliability of our estimates depends strongly on the validity of our assumption that in each electronic relaxation process at least one vibrational quantum is excited, or equivalently $\eta_0=0$. In Sec. V A we argued that this is a reasonable assumption, although it is not possible to verify it on the basis of the SRRS and ASRRS results. Still, one could explain the experiment by assuming that OH^- and OD^-, instead of having strongly different vibrational lifetimes, have a nonzero and different η_0. From expression (5.3) and the experimental values it is then derived that $(1-\eta_0)$ should be at least an order of magnitude smaller for OH^- than for OD^-, meaning that the E-V transfer is very inefficient. To achieve realistic values for the relative populations of the vibrational levels, one would then be forced to assume a much longer vibrational lifetime than was measured for the isolated OH^-. Also, one expects that η_0 is similar for OH^- and OD^-, because the static effects of these two ions are expected to be equal. Finally, we will show in the next paper, paper III, that the electronic relaxation rates for the $F_H(OH^-)$ and $F_H(OD^-)$ center are nearly identical, suggesting that they have a similar relaxation mechanism, and thus a nearly identical η_0.

Therefore we conclude that the vibrational lifetime is indeed much longer for OD^- than for OH^-, and also that it is temperature independent. A temperature-independent vibrational relaxation has also been established for the unperturbed OH^- impurity.[14,30] For KBr:OH^- a vibrational lifetime of 7 ns has been measured, close to the one we observe for the $F_H(OH^-)$. But the isotope effect for the unperturbed impurity seems to be different: The relaxation time for KCl:OD^- (3 ns) is only slightly larger than for KCl:OH^- (2 ns),[30] in contrast to the difference of an order of magnitude that we observe in the case of the F_H center.

The features of the vibrational relaxation of both perturbed and unperturbed OH^- are clearly different from the behavior expected for decay into phonons. The latter is characterized by a strong temperature dependence, and the energy-gap law predicts an increase of the relaxation rate on deuteration, because fewer phonons are required to dissipate the vibrational energy. Experimental and theoretical work on diatomic impurities in noble-gas solids has shown that a *decrease* of the relaxation rate on deuteration can be found if the vibration decays into localized rotations of the impurity.[27,28,33–35] It has been proposed that the energy of the vibration is transferred to the highest accessible rotational state, with only a minimal contribution from phonons.[35] Because this high rotational level is not thermally populated over the entire studied temperature range, no dependence on temperature is expected from this process. The different effective-mass dependence of the level spacing for a (nearly) free rotator ($\sim\mu^{-1}$) with respect to the one of the stretching vibration ($\sim\mu^{-1/2}$) was the physical reason for the observed isotope effect in the noble-gas solids: for OD^- less rotational quanta are excited than for OH^- during the relaxation of a vibrational excitation. The model of Freed and Metiu,[33] which assumes a free rotator, predicts in our case a relaxation rate of OD^- that is 39 times slower than that of OH^-.

The rotation of the OH^- in alkali halides is definitely more strongly hindered than for the molecular impurities in the noble-gas solids and the rotational level spacing will be closer to the one of a librator ($\sim\mu^{-1/2}$). It has been argued that this is the reason for the nearly equal vibrational lifetimes for the unperturbed OH^- and OD^- in KCl.[30] The larger observed difference between OD^- and OH^- lifetimes in the F_H center could be attributed to a different spacing of the rotational levels than for the isolated ion, i.e., a difference in the potential which hinders the rotation. There is nothing surprising about this, for all models of the F_H center predict significant changes of the position of the molecule, compared to the position of the isolated one. And the studies of OH and NH relaxation in noble-gas solids reveal that the vibrational decay into rotations is highly sensitive to disturbances of the impurity site.

D. Nature of the *U* mode

The appearance at low temperatures of a mode at the frequency of the unperturbed stretch vibration suggests that it is related to impurities, which are not accompanied by an F center as close as in the F_H-center configuration. Because the position of the U mode coincides with that of the isolated impurities it cannot be observed with infrared absorption, and the electronic absorption of the associated F center is buried under that of the F_H centers. It has been observed that even before aggregation the F center-luminescence is reduced by 35% if 4.3×10^{-3} mol of OH^- are present in a sample. The reduction strongly increases with temperature, reaching 95% at 60 K.[8] These numbers clearly indicate that there is some interaction between F centers and OH^- impurities, at larger distances than the $\langle 200\rangle$ configuration of the F_H center. This is likely to be an E-V transfer process, but it does not need to be of the same nature as observed for the F_H center.

At higher temperatures the intensity of the U mode increases (Sec. IV A). This indicates that the $F_H(OH^-)$ center enters a state with a vibrational mode, that within the experimental resolution coincides with the true U mode. These are clearly vibrational modes of two different systems. That the low-temperature U mode is not directly related to F_H centers can be argued from its different concentration dependence. And in lowly doped samples the R and B modes are observed before optical conversion, which proves that there are

already some F_H centers, but there is no corresponding U mode. We will discuss here only the U mode that appears at low temperatures.

The vibrational excitation of the U mode after electronic excitation of the F center, as is witnessed by the ASRRS and SRRS spectra, raises the following questions: (i) Does the transfer of the F-center energy to the distant impurity sites occur directly by E-V transfer, which means that the distance between the F center and these impurity is still sufficiently small, or is the energy transfer indirect by V-V transfer from vibrationally excited F_H centers? (ii) Is the scattering from the U configuration nonresonant or resonant Raman scattering? In the latter case, again, one observes only impurities which are sufficiently close to interact with an F center.

After optimal conversion in the low doped sample [Fig. 7(c)] a ratio $U_{1,2}/U_{0,1}\sim 1$ is observed, which was zero in the quenched crystal. If the scattering were nonresonant from unperturbed impurities, which were vibrationally excited due to V-V transfer from vibrationally excited F_H centers after conversion, $U_{1,2}/U_{0,1}\sim 1$ means that 1/3 of the free OD^- impurities is vibrationally excited. Since the concentration of the unperturbed impurities is orders of magnitude larger than that of the F_H centers and since the OD^- vibration decays on a nanosecond time scale, this would imply a very efficient V-V transfer. Changing the V-V transfer efficiency by OD^--concentration variation would then change the distribution of the energy over the vibrational levels of the F_H center.[26] Measurements of the vibrational population of the F_H center with two strongly differing concentrations [Figs. 7(a) and 7(b)] showed that this was not the case.

The picture of the U mode we propose is therefore as follows. The F aggregation at 250 K does not only produce F_H centers, but also F-OD^- pairs with a larger separation. The Raman intensities $U_{v,v+1}$ $(v>0)$ are resonantly enhanced and are the result of direct E-V transfer between the distant F-OD^- pairs. The $U_{0,1}$ Stokes intensity is the sum of RRS from the distant F-OD^- pairs and nonresonant scattering from unperturbed OD^- impurities, because its intensity is somewhat weaker than the (nonresonant) scattering intensity of the unperturbed OD^- in an uncolored region of the crystal. The smaller intensity can be the consequence of absorption of the excitation beam by the F and F_H centers in the colored part of the sample. The nonresonant contribution should obviously be larger in the highly doped crystal, as is clear from the $\sim 10\times$ higher $U_{0,1}/B_{0,1}$ and $U_{1,2}/B_{0,1}$ [Fig. 7(c)] ratios in the highly doped than in the lowly doped sample after $F \rightarrow F_H$ conversion. The presence of a considerable resonantly enhanced contribution is clear from the 50% increase of the $U_{0,1}$ intensity after $F\rightarrow F_H$ conversion in the highly doped crystal (Fig. 1) and an increase by a factor of 3 in the low doped crystal. The F-OD^- pairs with larger separation are absent before conversion in the latter sample, as is concluded from the absence of the $U_{v,v\pm 1}$ intensities $(v>0)$. Both F_H centers and the distant F-OD^- pairs are present in the highly doped quenched crystal (cf. ASRRS of Fig. 1).

The concentration dependence of the $U_{v,v-1}/U_{1,0}$ intensity ratios, in contrast to the concentration independence for the R and B modes, indicates that the U mode probably represents an average of F-OD^- pairs with different separations, and not a single configuration. One can expect that the average distance between the F center and the impurity in the loosely bound pairs is concentration dependent. Because the E-V transfer efficiencies can be expected to be strongly dependent on the F-OD^- separation, the concentration variation for the U mode can be understood. An experimental problem is that the resonant Raman enhancement can be expected to be different for different F-OH^- distances. This makes a comparison with earlier luminescence-quenching or electronic relaxation measurements on unaggregated F-OH^- samples[8,36] very difficult. Our U mode observation could possibly be due to a relatively close pair of F center OH^- with a relatively small abundance, which only has a minor effect on the statistics of the F-center relaxation.

VI. SUMMARY

By means of a SRRS and ASRRS study of OH^- and OD^- modes, as observed under resonant excitation of F centers associated to these impurities, we identified several types of associations. We observed a U mode, which is interpreted by us as originating from F-OH^-/OD^- complexes at a wider distance than in the F_H center. These occur even before aggregation in crystals with a sufficiently high OH^- or OD^- concentration. Interactions between loosely associated F centers and OH^- had already been observed by means of luminescence quenching and ground-state recovery measurements.[7,8,36] The electronic absorption band is not affected. Our Raman spectra clearly show that their stretching mode is unshifted from that of the isolated molecular impurity, within 0.5 cm^{-1}, and that a rather efficient energy transfer into the $v=1$ and $v=2$ states of the molecule occurs.

We were also able to identify two stretching modes, R and B, attributed to the two configurations of the $F_H(OH^-)$ center, in which the F center and OH^- are at $\langle 200\rangle$ neighbor positions. In KBr, the R and B configurations are characterized by their bistable red- and blue-shifted electronic absorption bands, respectively. The identification agrees with the infrared vibrational absorption measurements of paper I. The Raman study is complicated by the efficient optical conversion between the two configurations. We concluded that at temperatures below 30 K the equilibrium between the red and blue configuration is determined mainly by the optical pumping of the system, but that above this temperature, the thermal reorientation process is dominant. We also observed phonon sidebands in the ASRRS spectrum of the R and B modes, which have a very different strength for OH^- and OD^-. The shape of the phonon sidebands is very similar to that of the SRRS spectrum of the F_H center, which is again similar to that of unperturbed F centers in KBr.

By studying the power dependence of the ASRRS intensities $I_{v,v-1}$ we determined the primary E-V energy-transfer efficiencies to the excited vibrational levels of the $F_H(OH^-)$ and the $F_H(OD^-)$ center. By using a simple model including some simplifying assumptions, one can conclude that the E-V transfer is essential mostly to the $v=1$ and $v=2$ states, with the highest quantum efficiency in $v=1$ for both OH^- and OD^-. This is in contrast to the results for $F_H(CN^-)$, for which it was found that a maximal amount of energy is involved in the E-V transfer, resulting in the excitation of three or four vibrational quanta.[6] The observed occupation of the higher v levels, up to $v=5$ for

OD^-, is due to a secondary process of repumping of vibrationally unrelaxed F_H centers. Despite the relatively short vibrational lifetime of OD^-, repumping occurs already at laser powers above 20 mW. In the case of OH^- higher power is necessary for repumping. From the repumping, with some assumptions, the vibrational lifetime τ_v was estimated to be of the order of 100 and 10 ns for OD^- and OH^-, respectively. The temperature independence of the vibrational lifetimes and the increase of the lifetime on deuteration suggest that the stretching mode decays into hindered rotations of the molecule, as is observed for diatomic impurities in solid noble-gas lattices. This vibrational decay mechanism in combination with the E-V transfer may be the origin of the optical conversion between the two configurations of the $F_H(OH^-)$ center in KBr.

At temperatures above 50 K the Raman lines of the F_H center disappear, in agreement with the vibrational absorption measurements of paper I. As a tentative explanation, we suggest that at these temperatures the molecule is less and less localized in bistable R and B configurations, and behaves like an oscillator with a frequency nearly unshifted from that of the isolated molecule. We will discuss the optical and thermal reorientation of the impurity ion in more detail in paper III, with the assistance of time-resolved measurements.

After ''over aggregation'' in the optical $F \rightarrow F_H$ conversion, the B and R modes decrease and several new modes (X, Y, and Z), appear in the SRRS and ASRRS spectra. This occurs particularly in samples with high OH^- and/or OD^- doping. We attribute these modes tentatively to the association of F centers to OH^- or OD^- defect pairs (studied extensively for isolated molecular defects). The observation of a strong ASRRS signal of the X and Y modes shows that efficient E-V transfer occurs again under electronic excitation of these defects.

All these observed U, R, B, X, Y, and Z modes show a fully parallel polarized Stokes and anti-Stokes resonant Raman spectrum. This has not yet been understood or analyzed. We will study the mechanism of the E-V energy transfer in the F_H center in paper III, after we have discussed our time-resolved measurements of the relaxation.

ACKNOWLEDGMENTS

Support by the NFWO (Belgian National Fund for Scientific Research), the IIKW (Interuniversitary Institute for Nuclear Sciences), and the Belgian Lotto is gratefully acknowledged. E.G. and M.L. would like to thank the NFWO for financial support, and F.L. wishes to thank the NSF for its support Grant No. DMR-92-23230. F.L. thanks his coworkers C.P. An and V. Dierolf for help measuring by FTIR the OH^- and OD^- concentrations in the used crystals.

[1] V. Dierolf and F. Luty, preceding paper, Phys. Rev. B **54**, 5952 (1996).
[2] E. Gustin, M. Leblans, A. Bouwen, and D. Schoemaker, following paper, Phys. Rev. B **54**, 6977 (1996).
[3] R.K. Swank and F.C. Brown, Phys. Rev. **130**, 34 (1963).
[4] S. Honda and M. Tomura, J. Phys. Soc. Jpn. **33**, 1003 (1972).
[5] Y. Yang and F. Luty, Phys. Rev. Lett. **51**, 419 (1983).
[6] F. Luty and V. Dierolf, in *Defects in Insulating Materials*, edited by O. Kanert and J.-M. Spaeth (World Scientific, London, 1993), Vol. 1, p. 17.
[7] L. Gomes and F. Luty, Phys. Rev. B **30**, 7194 (1984).
[8] L. Gomes and F. Luty, Phys. Rev. B **52**, 7094 (1995).
[9] H. Söthe, J.-M. Spaeth, and F. Luty, Radiat. Effects Defects Solids **119–121**, 269 (1991).
[10] H. Söthe, J.-M. Spaeth, and F. Luty, Rev. Solid State Sci. **4**, 499 (1990).
[11] H. Söthe, J.-M. Spaeth, and F. Luty, J. Phys. Condens. Matter **5**, 1957 (1993).
[12] D. Jang and J. Lee, Solid State Commun. **94**, 539 (1995).
[13] K. P. Koch, Y. Yang, and F. Luty, Phys. Rev. B **29**, 5840 (1984).
[14] C. E. Mungan, U. Happek, and A. J. Sievers, J. Lumin. **58**, 33 (1994).
[15] G. Halama, K. T. Tsen, S. H. Lin, F. Luty, and J. B. Page, Phys. Rev. B **39**, 13 457 (1989).
[16] G. Baldacchini, S. Botti, U. M. Grassano, L. Gomes, and F. Luty, Europhys. Lett. **9**, 735 (1989).
[17] B. Wedding and M. V. Klein, Phys. Rev. **177**, 1274 (1969).
[18] A. Afanasiev, C. P. An, and F. Luty, in *Defects in Insulating Materials* (Ref. 6), p. 551.
[19] G. Halama, S. H. Lin, K. T. Tsen, F. Luty, and J. B. Page, Phys. Rev. B **41**, 3136 (1990).
[20] G. Cachei, H. Stolz, W. von der Osten, and F. Luty, J. Phys. Condens. Matter **1**, 3239 (1989).
[21] F. Rong, Y. Yang, and F. Luty, Cryst. Lattice Defects Amorphous Mater. **18**, 1 (1989).
[22] J.F. Zhou, E. Goovaerts, and D. Schoemaker, Phys. Rev. B **29**, 5509 (1984).
[23] M. Leblans, W. Joosen, and D. Schoemaker, Phys. Rev. B **42**, 7220 (1990).
[24] C. E. Mungan (private communication).
[25] J. A. Koningstein, *Introduction to the Theory of the Raman Effect* (Reidel, Dordrecht, 1972).
[26] Y. Yang, W. von der Osten, and F. Luty, Phys. Rev. B **32**, 2724 (1985).
[27] L. E. Brus and V. E. Bondybey, J. Chem. Phys. **63**, 786 (1975).
[28] V. E. Bondybey and L. E. Brus, J. Chem. Phys **63**, 794 (1975).
[29] Y. Kondo and F. Luty, Solid State Commun. **40**, 325 (1981).
[30] C. E. Mungan, Ph.D. thesis, Cornell University, 1994.
[31] V. R. G. Dierolf and F. Luty, in *Defects in Insulating Materials* (Ref. 6), p. 559.
[32] S. Morato and F. Luty, Phys. Rev. B **22**, 4980 (1980).
[33] K. Freed and H. Metiu, Chem. Phys. Lett. **48**, 262 (1977).
[34] R. Englman, *Non-Radiative Decay of Ions and Molecules in Solids* (North-Holland, Amsterdam, 1979).
[35] R. B. Gerber and M. Berkowitz, Phys. Rev. Lett. **39**, 1000 (1977).
[36] D. J. Jang, T. C. Corcoran, M. A. El-Sayed, L. Gomes, and F. Luty, in *Ultrafast Phenomena V*, edited by G. R. Fleming (Springer-Verlag, Berlin, 1986).